Original Article

Stress Distribution and Displacement of Craniofacial Structures Following Force Application in Treatment of an Operated Bilateral Facial Cleft

Kunal V. Shet, M.D.S.;[1] K. Nillan Shetty, M.D.S.;[2,*] Rohan Rai, M.D.S.;[3] and Anurag D. Mahale, M.D.S.[4]

ABSTRACT
Objective: The purpose of this study was to analyze the stress distribution and displacement patterns within the craniofacial structures following application of transverse and anteriorly directed forces by means of rapid maxillary expansion and reverse pull headgear, respectively, using a finite element method in a patient with bilateral cleft.
Materials and Method: A finite element model was used to determine stress distribution and displacement of various craniofacial structures following application of transverse and anteriorly directed forces.
Results: Maximum forward displacement was 8.07 mm at the node corresponding to the incisal edge of the upper central incisor followed by 7.95 mm at the prosthion. Maximum positive displacement lateral displacement was 3.24 mm at the node representing the premolars. The lateral and medial pterygoid plates showed maximum superior movement of about 0.95 mm and 0.79 mm, respectively. In the dentoalveolar region, the stresses were highest in the apical region of the canine. In the maxilla, point A and ANS demonstrated higher stress values compared with previous studies; both inferior and superior surfaces demonstrated high stresses in the range of 10.11 to 10.20 kg/mm^2.
Conclusion: Although expansion can be achieved in adolescents, displacements are noted more in the structures located anteriorly and along the midline while the posterior and lateral structures demonstrate minimal displacement but high stresses. Rapid maxillary expansion must be used judiciously in adolescents because of its far-reaching effects involving heavy stresses noted at the sphenoid bone, zygomatic bone, nasal bone, and their adjacent sutures. (*Turkish J Orthod*. 2014;27:148–157)

KEY WORDS: Bilateral Cleft; FEM; Finite-element study

INTRODUCTION

Oral clefts are the most common form of congenital defects. The reported incidence of cleft palate (CP) is 1.15 per thousand and that of isolated cleft palate is 0.08 per thousand.[1] According to estimates, roughly 30,000 children are born with cleft lip CL/CP anomalies every year,[2] which brings a set of complex problems that have functional, esthetic, psychological, and psychosocial implications.

There are no simple solutions for approaching the myriad problems associated with the CL/CP patient. Through a team of experts, the required care and counseling can be provided to the child and parent.

As the advancement in providing basic care has increased, the quality of life of these patients has also increased. Improvement in esthetics can provide patients with CL/CP high self-esteem. Often, the scars left from surgery and poor speech persist throughout life. The resultant scar leads to retarda-

[1]Private practice, Mumbai, India
[2]Professor, Department of Orthodontics and Dentofacial Orthopedics, A.J. Institute of Dental Sciences, Mangalore, India
[3]Professor and Head of the Department, Department of Orthodontics and Dentofacial Orthopedics, A.J. Institute of Dental Sciences, Mangalore, India
[4]Resident, Department of Orthodontics and Dentofacial Orthopedics, A.J. Institute of Dental Sciences, Mangalore, India

*__Corresponding author:__ K. Nillan Shetty, Department of Orthodontics and Dentofacial Orthopedics, A.J. Institute of Dental Sciences, Kuntikana, Mangalore, India 575004. Tel: 91-9845278015 E-Mail: nillanshetty@yahoo.co.in

To cite this article: Shet KV, Shetty KN, Rai R, Mahale AD. Stress distribution and displacement of craniofacial structures following force application in treatment of an operated bilateral facial cleft. *Turkish J Orthod*. 2014;27:148–157 (DOI: http://dx. doi.org/10.13076/TJO-D-15-00007)
Date Submitted: January 2014. Date Accepted: March 2015.

Table 1. Material parameters used in the finite element model

Material	Young's Modulus, N/mm^2	Poisson's Ratio
Tooth	2.0×10^3	0.3
Cortical bone	1.37×10^3	0.3
Trabecular bone	7.9×10^2	0.3

tion of growth of the maxilla 3-dimensionally, leading to class III malocclusion due to hypoplastic maxilla and a relatively normal mandible. Such types of malocclusion require early intervention by means of growth modulation appliance during the prepubertal and/or pubertal growth spurt stages to correct the hypoplastic maxilla, thereby correcting the class III profile.[3] Studies have confirmed that the maxilla can be repositioned anteriorly by dissociation of circum-maxillary sutures using protraction forces.[4,5] One of the modalities of correcting the hypoplastic maxilla 3-dimensionally is by the use of rapid maxillary expander (HYRAX) and reverse pull headgear simultaneously in the transverse and sagittal planes, respectively.[6–10]

In the past decade, the application of a well-proven predictive technique originally used in structural analysis, the finite element method (FEM), has revolutionized dental biomechanical research.[11–16] The FEM is a numerical method of analysis that provides the orthodontist with the quantitative data that can extend the understanding of the physiologic reactions that occur and thus allows the study of stress distribution in biological systems.[17–23]

This method offers an accurate model of the tooth and its surrounding structures with its complicated geometry. It makes it possible to apply various forces analytically at any point and in any direction and also to assess quantitatively and qualitatively the distribution of such forces.

Thus, FEM arms us with a valuable and potent tool for investigating the effect of external forces on the morphology of various craniofacial structures.

The purpose of the current study was to analyze the stress distribution and displacement patterns within the craniofacial structures following application transverse and anteriorly directed forces by means of rapid maxillary expansion (RME) and reverse pull headgear, respectively, using the FEM in a bilateral cleft patient.

MATERIALS AND METHOD

In this study, an FEM was used to determine stress distribution and displacement of various craniofacial structures following application of transverse and anteriorly directed forces in an operated bilateral facial cleft patient.

The FEM study was carried out at the Mechanical Department of Manipal College of Technology, Manipal, India. The computer was an IBM machine with a Pentium i7 processor, 500 gb hard disk, 8 gb of RAM, and an onboard graphics accelerator card. The monitor was 17 inches wide with a refresh rate of 70 Hz. Initial geometric modeling was done with the HyperMesh modeling package. The FEM was done using MIMICS software for Windows 7. Appropriate material parameters were selected (Table 1) and forces were applied (Table 2). Steps involved in the finite element modeling are as follows (Figs. 1 through 5):

1. Construction of the geometric model
2. Conversion of the geometric model to finite element model
3. Material property data representation
4. Defining boundary conditions
5. Application of forces

The transverse forces used in the simulation model were forces typically seen in RME with HYRAX. The nodes of the midpalatal suture were left constrained. This helped with the study of stress distribution in the surrounding craniofacial structures following RME. A force of 500 g per side was applied in the direction of the midpalatal suture. Anteriorly directed forces of 400 g per side at an angle of 30° downward in relation to the occlusal plane were applied to simulate the action of a reverse pull headgear.

Table 2. Magnitude of force applied in the finite element method

Force Type	Force Magnitude	Direction
Transverse	500 g	Horizontal force in the transverse direction from midpalatal suture
Anterior	400 g/side	Anteriorly directed force at the angle of 30° to occlusal plane

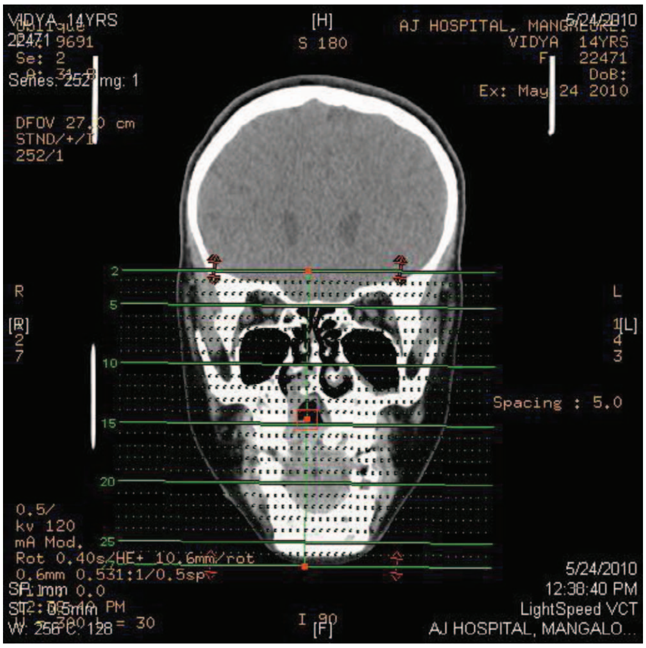

Figure 1. Computed tomography scan.

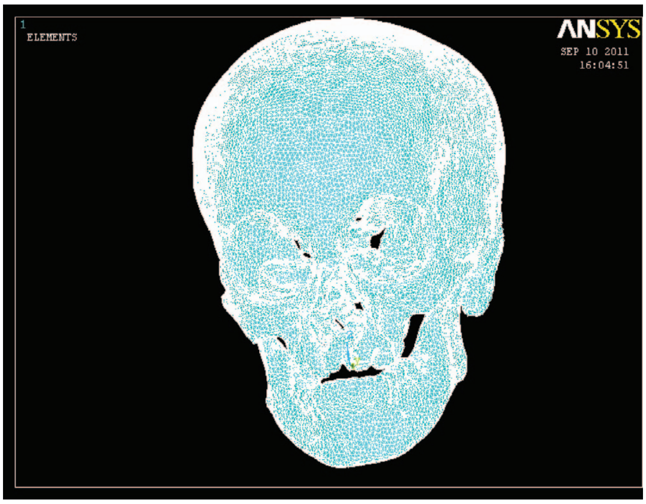

Figure 3. Elements and node.

RESULTS

Displacement of the craniofacial structures was studied in all 3 dimensions: transverse plane (Y), sagittal plane (X), and vertical plane (Z). A positive value (+) suggested an upward movement in the vertical plane (Z) and anterior movement in the sagittal plane (X). A negative value (–) indicated a posterior movement in the sagittal plane (X) and a downward movement in the vertical plane (Z; Table 3).

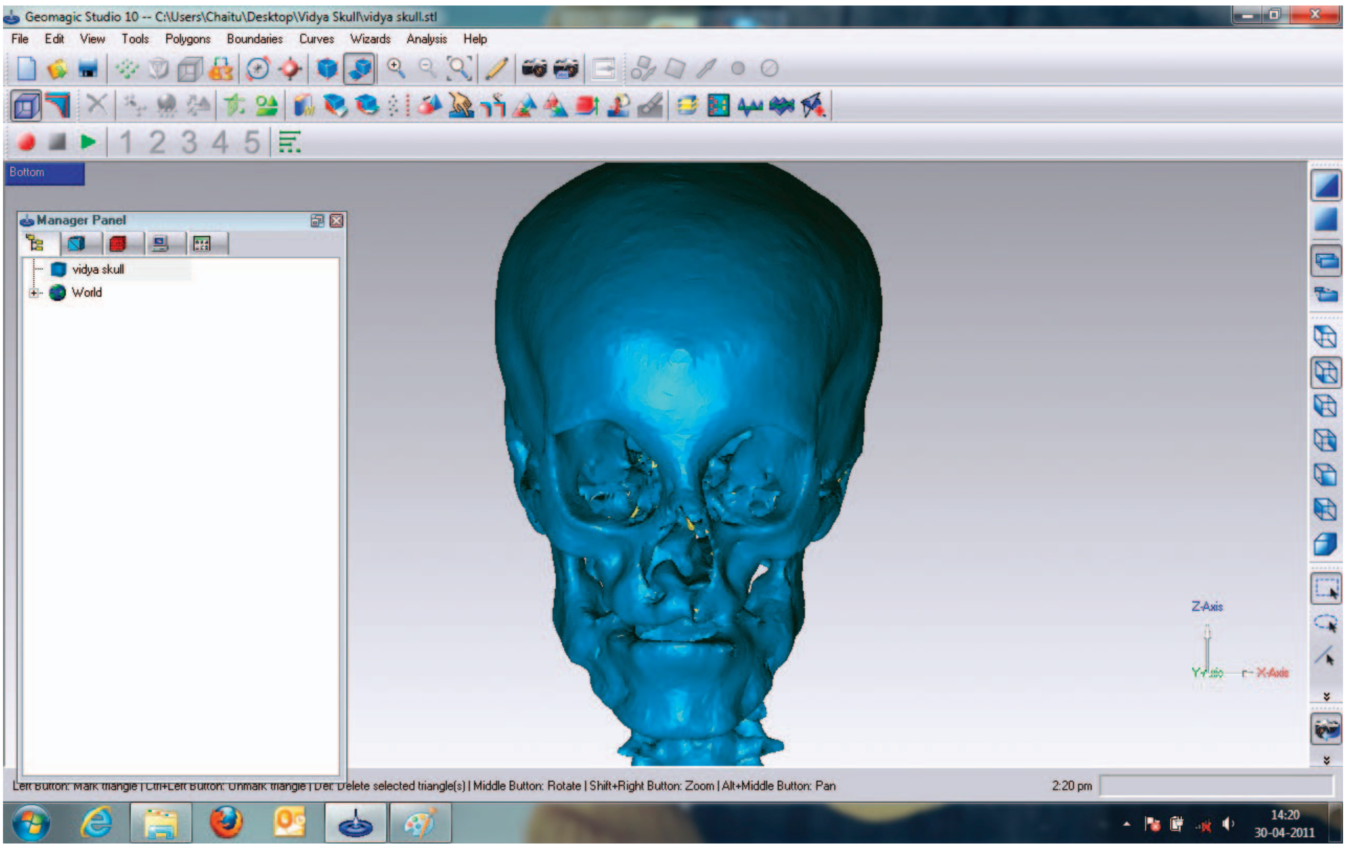

Figure 2. MIMICS.

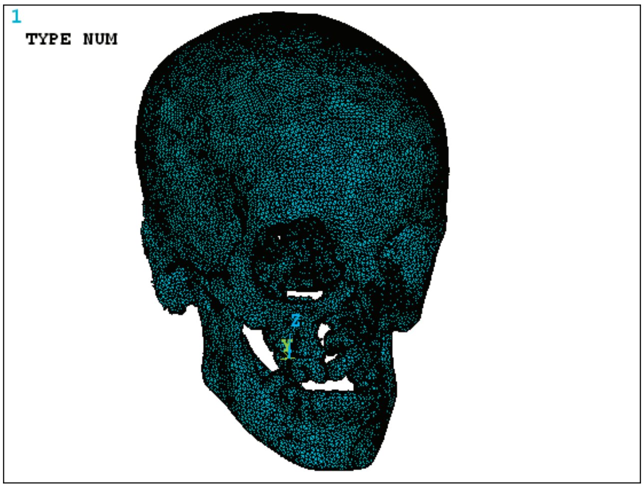

Figure 4. Meshing.

Displacement in the Anteroposterior Plane (X-Displacement)

The maximum X-displacement (forward displacement) was 8.07 mm at the node corresponding to the incisal edge of the upper central incisor followed by 7.95 mm at the prosthion. Displacements were noted more frequently in the dentoalveolar region compared with the skeletal structures. All of the dentoalveolar structures, maxillary structures, and structures of the nasal cavity wall demonstrated forward displacement to a varying extent. Preceding changes were evident only when 6 mm of prosthion advancement occurred (Figs. 6 through 9).

Displacement in the Transverse Plane (Y-Displacement)

The maximum positive (Y) displacement (lateral displacement) was 3.24 mm at the node representing the premolar, followed by canine, molar, and incisor teeth on both sides. Therefore, posterior expansion was greater compared with anterior expansion. From the frontal view, pyramidal displacement of the maxilla away from the midline was evident. At complete separation of the expansion

Table 3. Displacement pattern

	x-Axis, mm	y-Axis, mm	z-Axis, mm
Maxilla			
Point A	6.32	0.53	−0.9
ANS	5.83	1.06	−1.2
Prosthion	7.95	1.08	−1.6
Zygomatic buttress	2.78	0.25	−0.2
PNS	3.2	0.21	0.3
Inferior orbital rim	1.42	0.35	0.1
Nasal cavity wall			
Inferior	2.95	0.13	0.1
Superior	2.36	0.15	0.2
Nasal septum	2.38	0.1	0.15
Zygomatic bone			
Frontal	0.49	0.19	0.05
Temporal	0.81	0.19	0.03
Maxillary	0.9	0.21	0.02
Body	0.63	0.26	0.09
Frontal bone			
Zygomatic process	2.44	0.8	0.02
Supraorbital ridge	0.24	0.09	0.01
Sphenoid bone			
Lateral pterygoid	1.85	0.93	0.95
Medial pterygoid	2.46	1.12	0.79
Dentition			
Central incisor	8.07	1.05	−1.24
Canine	7.68	3.12	−1.92
Premolar	7.16	3.24	−1.01
Molar	6.5	1.89	−1.2

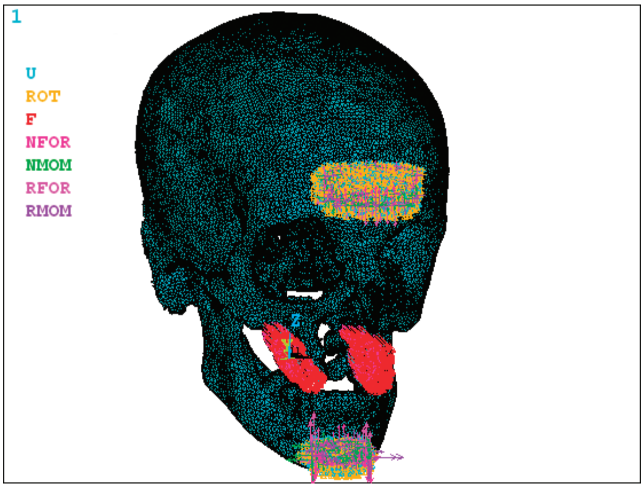

Figure 5. Boundary conditions.

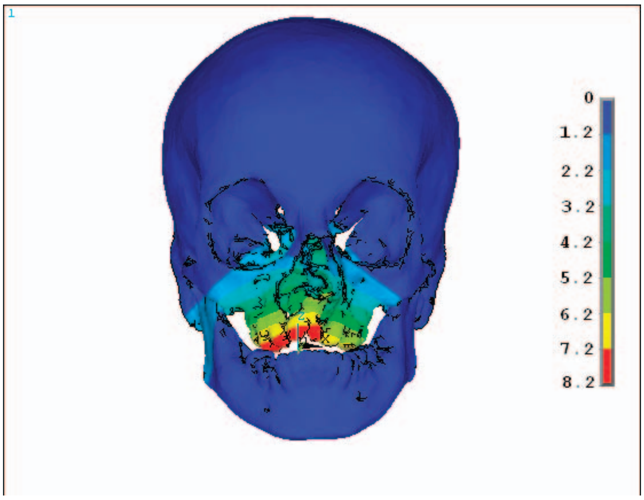

Figure 6. Displacement frontal view.

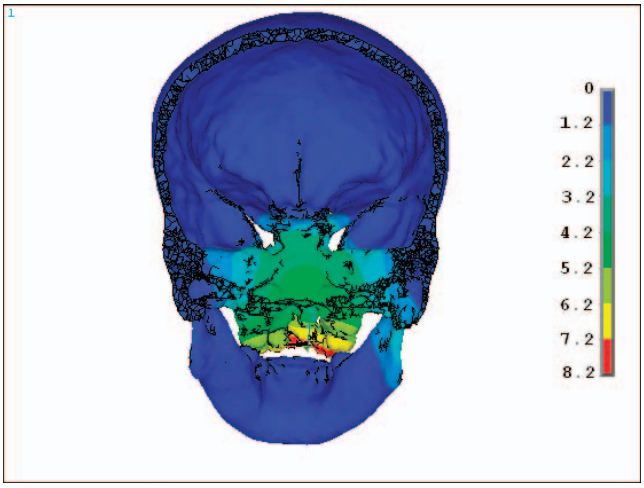

Figure 7. Displacement posterior view.

device, displacement of cranial bones was evident, and the width of the nasal cavity at the floor of the nose increased markedly, whereas the superior aspect of the same showed lesser lateral displacement. No significant displacement was observed at the zygomatic and frontal bone, except at the zygomatic process of the frontal bone, which moved laterally. Lateral and medial pterygoid plates showed a marked tendency for lateral displacement. Minimum displacement was observed in the region close to the cranial base, which may be attributed to rigid plates (Figs. 6 through 9).

Displacement in the Vertical Plane (Z-Displacement)

The lateral and medial pterygoid plates showed maximum superior movement (+Z-displacement) of about 0.95 mm and 0.79 mm, respectively. Maximum downward displacement (–Z-displacement) was 1.92 mm at the node representing the canine followed by incisors, molars, and premolars. Also, point A, prosthion, and ANS showed an anterior movement, suggesting that the nasomaxillary complex rotated in such a manner that the lateral structures moved upward and the midline structures moved downward (Figs. 6 through 9).

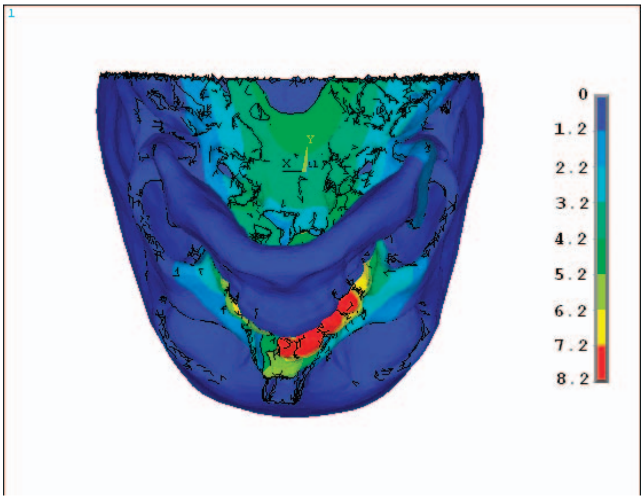

Figure 9. Displacement pattern inferior view.

Comparison of Maximum Von Mises Stresses on Various Structures of the Craniofacial Complex With Varying Amount of Expansion and Anterior Protraction (Table 4)

Stress images of the 3-dimensional model of the skull are shown. The areas of stress are shown with the help of different colors. The pellets of colors representing the tensile and compressive stresses are shown on right side of the diagram. In the dentoalveolar region, the stresses were highest in the apical region of the canine followed by that of

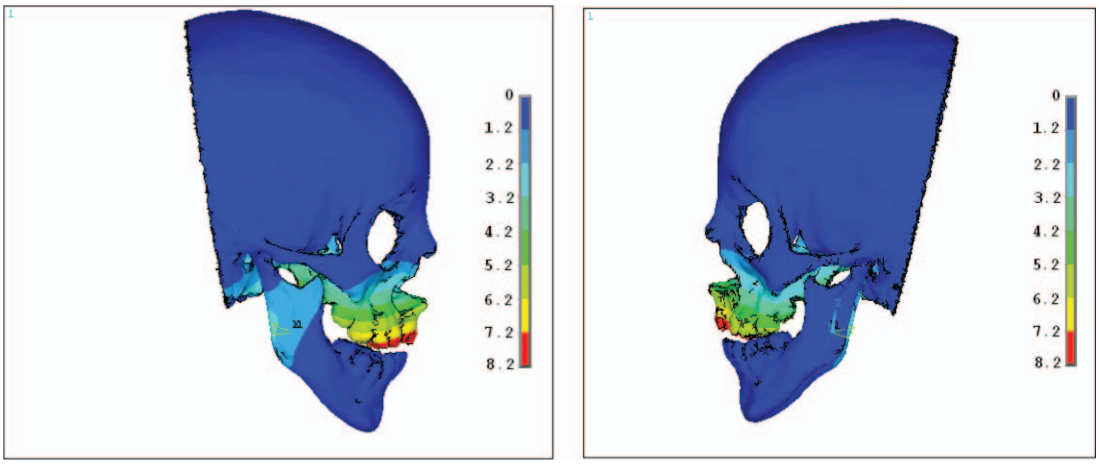

Figure 8. Displacement lateral view.

Table 4. Stress distribution pattern

	Von Mises Stress, N/mm^2
Maxilla	
Point A	7.31
ANS	7.12
Prosthion	2.71
Zygomatic buttress	2.9
PNS	2.43
Inferior orbital rim	2.32
Nasal cavity wall	
Inferior	10.2
Superior	10.11
Nasal septum	9.82
Zygomatic bone	
Frontal	8.92
Temporal	4.9
Maxillary	9.21
Body	7.56
Frontal bone	
Zygomatic process	2.4
Supraorbital ridge	2.12
Sphenoid bone	
Lateral pterygoid	7.61
Medial pterygoid	8.14
Dentition	
Central incisor	12.72
Canine	18.82
Premolar	13.41
Molar	13.79

molars and premolars. In the maxilla, point A and ANS demonstrated higher stress values compared to previous studies, and both inferior and superior surfaces demonstrated high stresses in the range of 10.11 to 10.20 kg/mm^2. The zygomatic bone and sphenoid bone showed a high level of stress, especially in the maxillary process of the zygomatic bone, whereas the frontal bone showed minimal values of stress (Figs. 10 through 14).

DISCUSSION

Finite element analysis is a mathematical method in which the shape of complex geometric objects and their physical properties are computer constructed. Interactions of various components of the model are then calculated for stress, strain, and deformation. This was first used in orthodontics by Thresher and Saito[18] to study stresses in human teeth. Ever since, this method has proved effective in simulation of tooth movement and optimization of orthodontic mechanics. Extensive use has been primarily done because the method is noninvasive; the actual amount of stress experienced at any given point can be theoretically measured; the structures of the craniofacial complex can be visualized graphically; the point of application, magnitude, and direction of force may easily be varied to simulate clinical situations; reproducibility does not

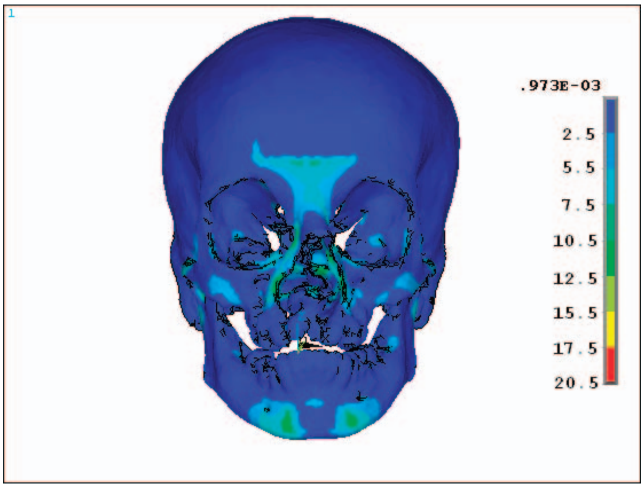

Figure 10. Stress pattern frontal view.

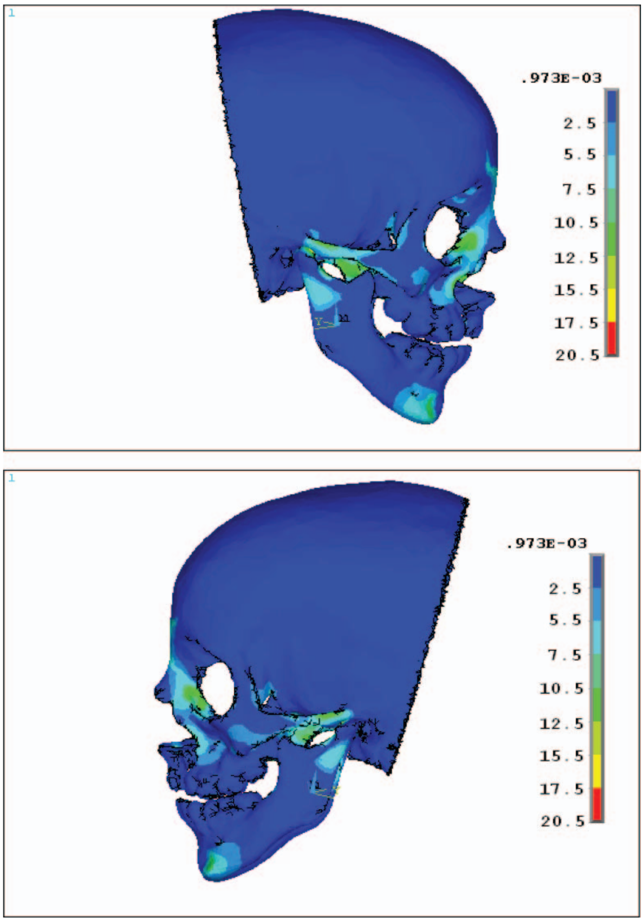

Figure 11. Stress pattern lateral view.

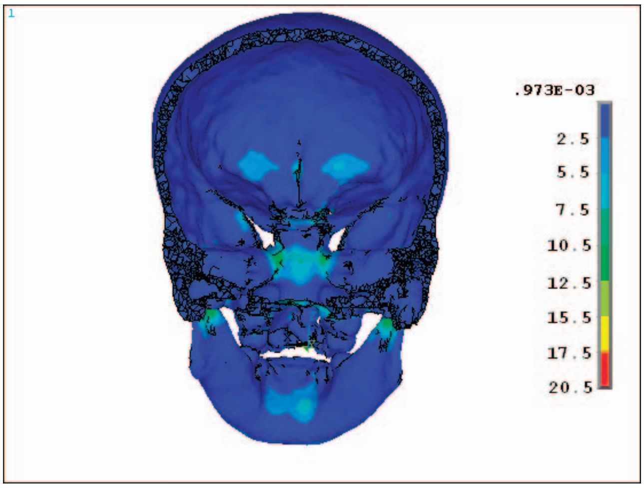

Figure 12. Stress pattern posterior view.

affect the physical properties of the involved material; and the study can be repeated as many times as the operator wishes.

The 3-dimensional FEM used in the present study provided the freedom to simulate orthodontic force systems applied clinically and allowed analysis of response of the craniofacial skeleton to the orthodontic loads in 3-dimensional space.

The pattern of displacement revealed that the greatest widening was observed in the dentoalveolar structures, with the expansion effect gradually decreasing toward the superior skeletal structures. The results of the present study support those of previous studies.[24,25]

In the sagittal (Y) plane, the structures along the midline showed an anterior displacement, while lateral structures demonstrated a posterior displacement.

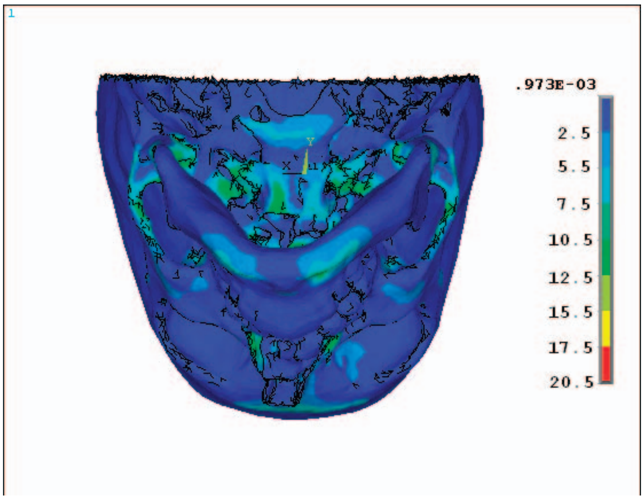

Figure 13. Stress pattern inferior view.

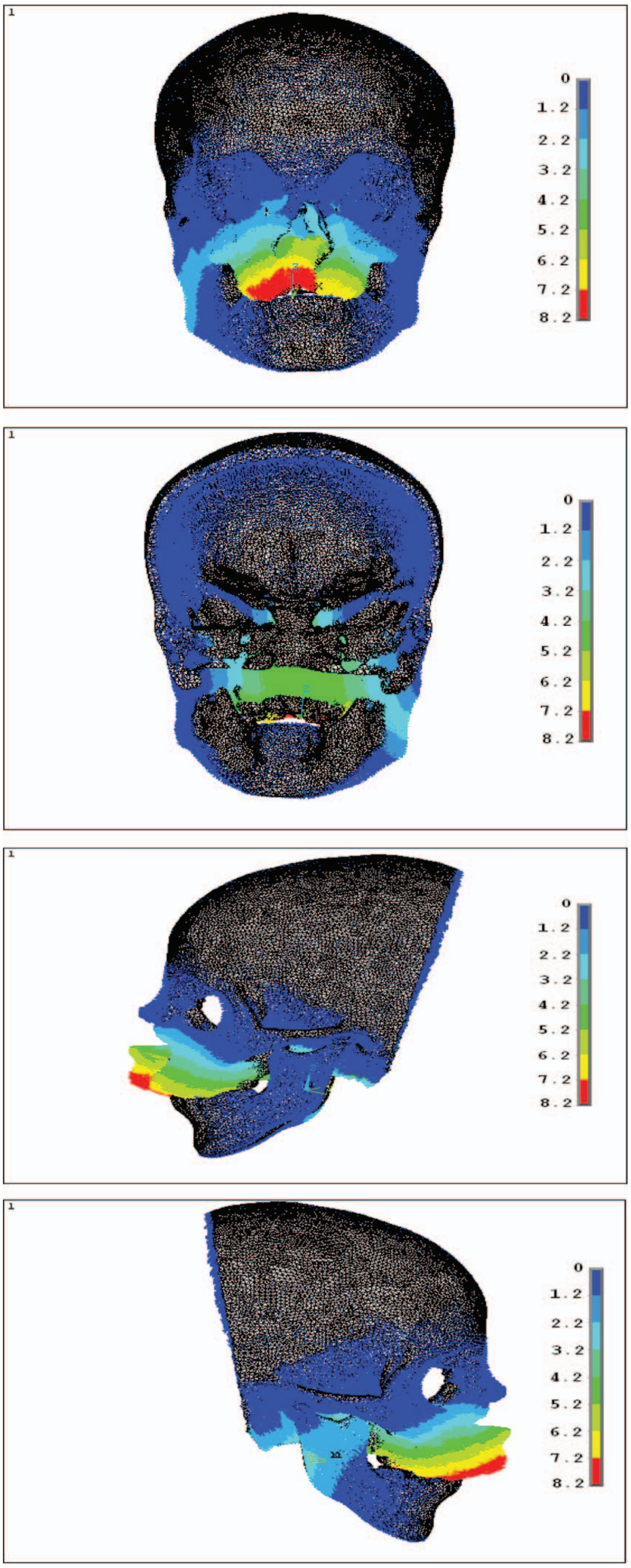

Figure 14. Vector deformation.

In the vertical (Z) plane, the entire maxillary complex descended downward more or less in a parallel manner while the lateral structures demonstrated an upward displacement.

A composite skull model was used for FEM analysis. In response to RME, an asymmetric expansion pattern was noted for the 2 halves of the maxilla. This asymmetric and unpredictable movement of the 2 halves was also observed for other maxillary articulations, such as the zygomatic and sphenoid bones. The expansion was simulated in a patient model with bilateral cleft deformity of palate and alveolus. The typical wedge-shaped opening in the anteroposterior plane seen in noncleft patients[24,25] as a result of RME was not seen in the present study. It was observed that the expansion in the canine region was greatest as compared with the posterior region, unlike in previous studies.[22,23]

This could be related to the presence of cleft of the secondary palate. Also, the expansion on the cleft patient occurs in the osseous defects between the premaxilla and the maxilla or at the incisive suture region, rather than at the intemaxillary suture, as occurs in normal patients.

The nasomaxillary complex and teeth were displaced. Thus, expansion therapy in CL/CP along with maxillary protraction helps to reduce deformity. The lateral displacement of the borders of the piriform aperture clearly demonstrated an increase in nasal cavity width.

The present study revealed maximum lateral displacement in the canine region, which was in contrast to the study done by Gautam and coworkers,[22] in which the maximum lateral displacement for maxillary teeth was observed at the second molar followed by first molar, second premolar, canine, and lateral incisor. The probable reason may be the simultaneous force application in the anteroposterior and transverse plane, unlike the previously mentioned study, in which forces were applied in the transverse plane only.

Maximum inferior movement was noted in the canine and premolar region followed by the molars and was minimum in the incisors, which was in contrast to a previous study[19] in which incisor extrusion was greatest compared with that of the second molar. In all probability, this was due to the 30° downward angulation of the force vector, and the point-of-force application was at the canine fossa region in the anteroposterior plane.

An anterolateral movement of zygomatic bone was observed in contrast to a previous study,[20] in which zygomatic bone showed posteromedial movement. This change in the direction of movement of zygomatic bone was because a face mask was used in conjunction with RME in the current study vs a headgear used for maxillary growth restriction in the previous study.

The investigators noted frontal bone movement in an anterolateral and superior direction, in contrast to the study by Baldawa and Bhad,[23] in which frontal bone did not show any displacement. This could be attributed to higher forces in the anteroposterior and transverse planes.

It was observed that all the structures of the maxilla had a lateral displacement with RME and face mask therapy, which is in agreement with findings of existing scientific evidence.[17,19,21,22]

The current investigators noted lateral and anterior displacement of medial and lateral pterygoid plates. This contradicted the findings of Gautam *et al*.[19] However, the findings were in unison with another study conducted by Gautam *et al*.[22] The opening of the palatal sutures was seen to be more pronounced in the anterior region and decreased progressively toward the posterior region, which was in sync with previous studies. This mainly stemmed from the use of RME for lateral expansion in all the studies.

The increase in nasal cavity width at the floor of the nose was in conjunction with the previous studies.[17,22] It was observed that the superior region of the nasal cavity moved laterally. The nasal bone moved laterally and anterosuperiorly with face mask therapy, in stark contrast to a previous study.[23] Baldawa and Bhad[23] reported a medial movement of the nasal bone. These notable differences were due to the different modalities of force application.

The area of inferior nasal cavity wall point A and ANS region showed high stress. This region corresponds to subtotal Le Fort I osteotomy. These regions act as source of resistance to expansion.[19,20] The pterygomaxillary articulation showed areas of high stress. The restriction to lateral bending led to higher Von Mises stress at medial pterygomaxillary articulation. Hence, the previous findings[19–22] that the connection between the maxilla and the pterygoid plate of the sphenoid bone, regardless of the presence of the midpalate, is one of the sites of major resistance to expansion were partly supported by the present study. In view of this finding, one can argue against the need for lateral pterygomaxillary disjunction during the surgically assisted rapid palatal expansion (SARPE) procedure in clefts involving the secondary palate. Because of the presence of the cleft, the center of rotation in all 3 planes of space was located close to the canine region.

Even though FEM is a powerful research tool, it has its limitations. The success of FEM studies depends on the accuracy of the created models. Accurate modeling, in turn, depends on the accuracy of the input data and its consequent processing. As the FEM model is based on these predetermined values, it fails to take into account factors such as bone elasticity that can differ between individuals and that may alter with age. Computed tomography (CT) scans are used in most cases to create finite element models of biological systems. A CT scan of even 1-mm sections cannot accurately represent periodontal ligament and teeth because of their different physical properties.[26–28] This further leads to inaccuracies in the finite element model, which might not adequately demonstrate the transfer stresses. Taking these shortcomings into account, other research methodologies may be required for better visualization of changes in these structures.

CONCLUSION

It can thus be concluded from the present study that:

- All the structures of the maxilla had lateral displacement with RME and face mask therapy.
- Greatest widening was observed in the dento-alveolar structures, with the expansion effect gradually decreasing toward the superior skeletal structures.
- An asymmetric expansion pattern was noted for the 2 halves of the maxilla without the typical wedge-shaped opening in the antero-posterior plane seen in noncleft patients
- Expansion therapy in CL/CP along with maxillary protraction helps to reduce deformity due to displacement of the nasomaxillary complex and the teeth.
- The study noted that the maximum lateral and inferior displacement was observed in the canine region.
- As expected, an increase in nasal cavity width was noted.
- The pterygomaxillary articulation is a site of major resistance to maxillary expansion, and its need for its disjunction during SARPE is recommended for procedures involving the secondary palate in cleft patients.

REFERENCES

1. Kumar B, Shetty V, Valiathan A. Incidence of cleft lip & palate in Manipal in the past decade. *J Ind Orthod Soc*. 1998;31:99–102.
2. Kharbanda OP. *Abstract Book 11th Postgraduate Convention of the Indian Orthodontic Society*. New Delhi, India: All India Institute of Medical Sciences; 2007.
3. Franchi L, Baccetti T, McNamara JA Jr. Post-pubertal assessment of treatment timing for maxillary expansion and protraction therapy followed by fixed appliances. *Am J Orthod Dentofac Orthop*. 2004;125:555–568.
4. Kambara T. Dentofacial changes produced by extraoral forward forces in the Macaca irus. *Am J Orthod*. 1977;71: 249–277.
5. Nanda R. Protraction of maxilla in rhesus monkey by controlled extraoral forces. *Am J Orthod*. 1978;74:121–142.
6. Petit HP. Adaptation following accelerated facial mask therapy. In: McNamara JA Jr, Ribbens KA, Howe RP, eds. *Clinical Alterations of the Growing Face. Monograph 14, Craniofacial Growth Series*. Ann Arbor, MI: Center for Human Growth and Development; University of Michigan; 1983.
7. Baik HS. Clinical results of the maxillary protraction in Korean children. *Am J Orthod Dentofacial Orthop*. 1995; 108:583–592.
8. Macdonald KE, Kapust AJ, Turley PK. Cephalometric changes after the correction of Class III malocclusion with maxillary expansion/facemask therapy. *Am J Orthod Dentofacial Orthop*. 1999;116:13–24.
9. McGill JS, McNamara JA Jr. Treatment and post-treatment effects of rapid maxillary expansion and facial mask therapy. In: McNamara JA Jr, ed. *Growth Modification: What Works, What Doesn't and Why. Monograph 36, Craniofacial Growth Series*. Ann Arbor, MI: Center for Human Growth and Development, University of Michigan; 1999.
10. Westwood PV, McNamara JA Jr, Baccetti T, Franchi L, Sarver DM. Long-term effects of Class III treatment with rapid maxillary expansion and facemask therapy followed by fixed appliances. *Am J Orthod Dentofacial Orthop*. 2003; 123:306–320.
11. Miyasaka-Hiraga J, Tanne K, Nakamura S. Finite element analysis for stresses in the craniofacial sutures produced by maxillary protraction forces applied at the upper canines. *Br J Orthod*. 1994;21:343–348.
12. Tanne K, Matsubara S, Sakuda M. Location of the center of resistance for the nasomaxillary complex studied in a 3-D finite element model. *Br J Orthod*. l995;22:227–232.
13. Tanne K, Matsubara S. Association between the direction of orthopedic headgear force and sutural responses in the nasomaxillary complex. *Angle Orthod*. 1996;66(2):125–130.
14. Cobo J, Arguelles J, Puente M, Vijande M. Dentoalveolar stress from bodily tooth movement at different levels of bone

loss. *Am J Orthod Dentofacial Orthop*. 1996;110(3): 256–262.

15. Koriotb TW, Versluis A. Modeling the mechanical behavior of the jaws and their related structures by finite element (FE) analysis. *Crit Rev Oral Biol Med*. 1997;8(1):90–104.
16. Iseri H, Tekkaya AE, Oztan O, Bilgic S. Biomechanical effects of rapid maxillary expansion on the craniofacial skeleton, studied by the finite element method. *Eur J Orthod*. 1998;20(4):347–356.
17. Jafari A, Shetty KS, Kumar M. Study of stress distribution and displacement of various craniofacial structures following application of transverse orthopedic forces—a three-dimensional FEM study. *Angle Orthod*. 2003;73(1):12–20.
18. Thresher RW, Saito GE. The stress analysis of human teeth. *J Biomech*. 1973;6(5):443–449.
19. Gautam P, Valiathan A, Adhikari R. Skeletal response to maxillary protraction with and without maxillary expansion: a finite element study. *Am J Orthod Dentofacial Orthop*. 2009; 135:723–728.
20. Gautam P, Valiathan A, Adhikari R. Craniofacial displacement in response to varying headgear forces evaluated biomechanically with finite element analysis. *Am J Orthod Dentofacial Orthop*. 2009;135:507–515.
21. Lee H, Ting K, Nelson M, Sun N, Sung SJ. Maxillary expansion in customized finite element method models. *Am J Orthod Dentofacial Orthop*. 2009;136:367–374.
22. Gautam P, Zhao L, Patel P. Biomechanical response of the maxillofacial skeleton to transpalatal orthopedic force in a unilateral palatal cleft. *Angle Orthod*. 2011;(81)3:507–515.
23. Baldawa RS, Bhad WA. Stress distribution analysis during an intermaxillary dysjunction: a 3D FEM study on an adult human skull. *J Ind Orthod Soc*. 2011;45(2):75–81.
24. Haas A. Rapid expansion of the maxillary dental arch and nasal cavity by opening the mid palatal suture. *Angle Orthod*. 1961;31:73–89.
25. Bishara SE, Staley RN. Maxillary expansion: clinical implications. *Am J Orthod Dentofacial Orthop*. 1987;91:3–14.
26. Tanne K, Sakuda M, Burstone CJ. Three-dimensional finite element analysis for stress in the periodontal tissue by orthodontic forces. *Am J Orthod Dentofacial Orthop*. 1987; 92:499–505.
27. Santler G, Karcher H, Ruda C. Indication and limitations of three-dimensional models in cranio-maxillofacial surgery. *J Craniomaxillofac Surg*. 1998;26:11–16.
28. Gateno J, Xia J, Teichgraeber JF, Rosen A. A new technique for the creation of a computerized composite skull model. *J Oral Maxillofac Surg*. 2003;61:222–227.